

VERIFICATION OF BEHAVIOR FACTORS THROUGH TIME-HISTORY NONLINEAR ANALYSIS

J. I. Ezeberry Parrotta¹, G. Hanna², D. Combescure³

¹ Technical Lead, IDOM, Madrid, Spain (jezeberry@idom.com)

² Technical Officer, Fusion for Energy (F4e), European Commission, Barcelona, Spain
(Gaston.Hanna@f4e.europa.eu)

³ Technical Officer, Fusion for Energy (F4e), European Commission, Barcelona, Spain
(Didier.Combescure@f4e.europa.eu)

ABSTRACT

This paper extends the previous study on the seismic design of reinforced concrete (RC) frame structures within the ITER project, focusing specifically on the validation of behavior factors (q) through nonlinear dynamic time-history analyses. While the prior work combined linear elastic methods and nonlinear pushover analyses, the present study emphasizes the detailed evaluation of structural response under realistic seismic loading conditions. Using SAP2000, extensive nonlinear time-history simulations are conducted to assess the validity of the behavior factor assumptions previously derived from pseudo-static (pushover) analysis.

The research specifically addresses a representative RC building, characterized by complex load paths and structural arrangements typical of critical facilities. By exploring various nonlinear modelling strategies—including traditional plastic hinges (ASCE 41-17) and fiber-based hinges (Fiber P-M2-M3) with different stiffness degradation parameters—the analyses quantify local ductility demands, hinge formation patterns, and global energy dissipation capabilities.

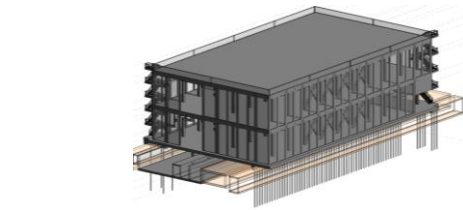
Results indicate that while the average behavior factors obtained from dynamic analyses closely align with previous pushover estimates, localized demands occasionally exceed elastic predictions ($q < 1$), highlighting regions requiring special design attention. Fiber-based models generally produce higher q -values due to enhanced energy dissipation capabilities and distributed plasticity effects. Additionally, sensitivity analyses varying the damping ratios confirm the limited influence of damping assumptions, as inelastic deformation predominantly governs the structural response.

This comprehensive dynamic assessment reinforces the appropriateness of adopting a conservative behavior factor ($q \leq 2$) in the conceptual seismic design of ITER-like RC structures. Furthermore, it underscores the necessity of integrating advanced nonlinear dynamic evaluations into the design process for critical nuclear facilities, ensuring robust structural resilience under seismic events.

INTRODUCTION

The purpose of this paper is to reinforce the methodology followed for the conceptual design of new reinforced concrete (RC) buildings in the ITER project under seismic loads. In a previous paper [Ezeberry Parrotta, et al], the classical approach based on linear-elastic analyses was complemented by the recommendations of Eurocode 8, which permits the use of the “Behavior Factor” (q) concept. This approach allows a reduction in seismic loads proportional to the structure’s ductility. This classical methodology based in a non-linear pseudo-static analysis implies a strong simplification in which the design spectrum is reduced by the value q in the zone of significant frequencies, and the reinforcement determined by means of linear-elastic dynamic analyses. Thus, to ensure both safety and structural integrity during seismic events, it is important to verify the validity of this assumption, and this is the reason of this paper. Based in non-linear time-history analysis, the actual behavior factor is computed along the structure, in the critical zones of beams and columns.

The analysis in this paper focuses on the Building #18, whose dimensions are presented in Figure 1. This building is founded on a soft soil adding complexity to the design. The results obtained by pushover analyses [Ezeberry Parrotta, et al] has demonstrated that the behavior factor must be limited to $q \leq 2$.



Dimensions: 37×66×22 (Width×Length×Height in meters)

- Level B1: - 4.000 m (Foundation slab)
- Level L1: + 0.000 m (Floor slab)
- Level L2: + 9.000 m (First level slab)
- Level R1: +18.000 m (Roof)

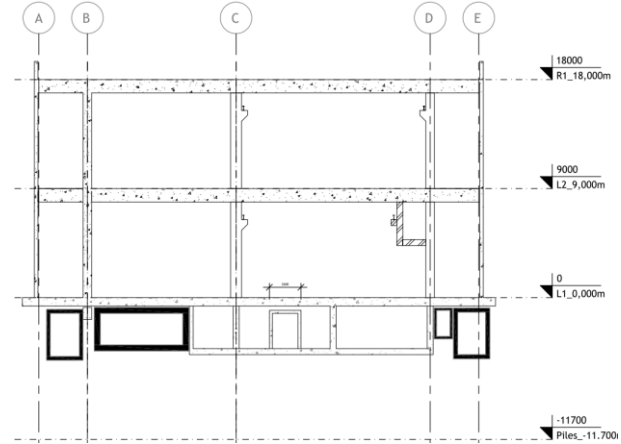


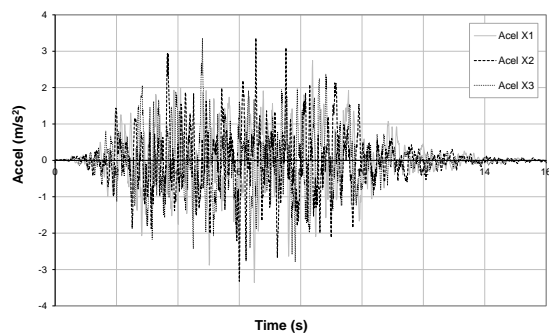
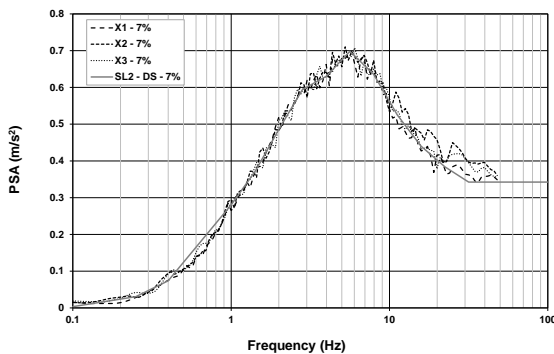
Figure 1. Buildings #18.

METHODOLOGY

Generation of Design Spectrum compatible time-histories signals

The first step in this process is the generation of Design Spectrum compatible signals valid for time-history analyses. The signals are computed with the program P-CARES [NUREG/CR-6922]. The methodology is based in the Shake-91 [Idriss et al], and the plots and main parameters are presented in Figure 2. In line with the ITER project [I-LSSR], three artificial ground motion time histories are generated for horizontal response. The vertical response is computed by applying a factor of 2/3. The design parameters for the generation of the time histories are:

- Time history duration: > 20 s according to NUREG-0800 Section 3.7.1.
- Time increment: < 0.10 s according to NUREG-0800 Section 3.7.1.
- Earthquake magnitude: $M_w = 7$ as it is the maximum magnitude expected for the ITER site.



Miscellaneous Parameters			
Iterations:	10	T_{rise} [s]:	3
T_{max} [s]:	20.48	T_{strong} [s]:	6
Data Points:	2048	T_{decay} [s]:	11
EQ Magnitude (M_w):	7		

Parameter\signal	X1	X2	X3
max I_A [m/s^2]	24.47	23.65	23.26
5% max I_A [m/s^2]	1.22	1.18	1.16
75% max I_A [m/s^2]	18.35	17.73	17.44
$T_{5\%}$ [s]	1.23	1.24	1.31
$T_{75\%}$ [s]	4.10	3.99	3.94
T_{sm} [s]	2.87	2.75	2.62

Figure 2. Time-histories generation plots and parameters.

Moreover, the following design requirements are followed according to NUREG-0800 Section 3.7.1:

- Each of the three time-histories shall be statistically independent from the others with the absolute value of their correlation coefficient below 0.16 (Appendix F of RG 1-208),
- The strong motion duration is defined as the time required for the Arias Intensity to rise from 5 percent to 75 percent. The minimum acceptable strong motion duration is 6 seconds.
- The average response spectra generated for each time histories shall not exceed the target response spectrum at any frequency by more than 30 percent and shall not fall more than 10 percent. Moreover, the average response spectra within a window frequency of no larger than +/- 10 percent centered on the frequency shall no fall below the target response spectrum.

Following the Appendix F of RG 1-208, the obtained correlation between signals are for X1-X2 equals 0.02, for X1-X3 equals 0.06, and for X2-X3 equals -0.05.

Material properties

Material parameters for the buildings are taken in accordance with the ITER regulation [I-SDCB] and Eurocodes 2 and 8. Structural concrete strength is $f_{ck} = 40$ MPa (C40/50). Reinforcing steel characteristic strength is $f_{yk} = 500$ MPa (B500SD). Soil properties are taken from the geotechnical study [I-SIR]. Limestone rock is found at a depth of 4.00 m (bottom of existing galleries). Its static Young's modulus is 150 MPa, Poisson's ratio is 0.20, friction angle 30° , and no cohesion is considered.

Damping will be taken according to RG 1.61. For SL-2 (SSE) seismic events, $\xi = 7\%$ is adopted for concrete structures. It must be noted that this damping is recommended for linear elastic analysis, whereas for non-linear analysis, in the case of plastic hinges, it is recommended to use a lower value to prevent double counting damping. Strictly speaking, this value should be calibrated in order to obtain the same global damping of 7%, however, due the simplified approach followed in conceptual design, it is decided to compare the results obtained with different lower values (i.e., 4-5%).

Finite Element Model

Plane Finite Element Models were created using SAP2000 software, with beam elements representing columns, transverse walls, beams and slabs. Non-structural mass was incorporated by assigning linearly distributed mass to the beam elements. The same finite element used for pushover analysis [Ezeberry Parrotta, et al] model is used, where nonlinear material properties—accounting for concrete and steel stress-strain curves per Eurocode 2—are introduced. Because the model uses beam elements, these nonlinearities appear only in the cross-sectional normal strains (Navier hypothesis), while shear-related nonlinearities are not directly included. Figure 3 shows the nonlinear constitutive equations for concrete (C40/50) and steel (B500S).

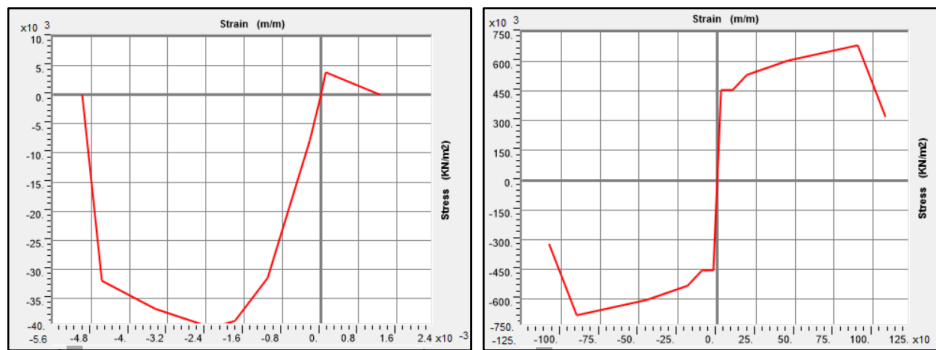
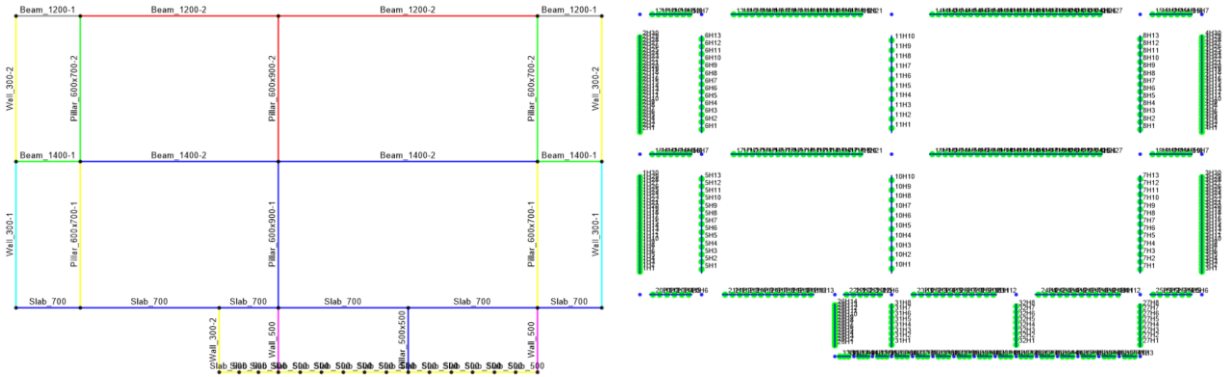


Figure 3. Non-linear constitutive equation for concrete (left) and steel (right)

A key step is defining plastic hinges in SAP2000, which provides specific hinge assignment methods for beams, columns, and foundations. As indicated in the previous paper [Ezeberry Parrotta, et al], two different hinge configurations were used for pushover analysis: Equal Spacing, where the hinges are distributed uniformly, and Non-linear Beam-Column Hinges, where the plastic hinges are located at the ends of the elements (classical approach). It was concluded that the Equal Spacing configuration is the best choice for this analysis.

SAP2000 can auto-define these hinges according to ASCE 41-17 for beams (Table 10-7), and columns (Table 10-8). For beams, the hinge properties typically consider bending (M3) and shear (V2), while neglecting axial force (N). On the other hand, for column hinges we must consider axial-moment (P-M3) interaction, reflecting how axial loads affect ductility. Finally, for foundation slabs, continuous spring supports can capture nonlinear foundation response in compression (and zero tension resistance), ensuring realistic load-transfer modelling.

This model was selected to accomplish the pushover analysis, and it is the reference Non-Linear (NL) model for this paper. Figure 3 shows the FEM for Buildings #18, showing the Frame sections (left) and the Hinges configuration (right).



Thickness Beam and columns elements: B#18 = 0.60 m
 Distance between frames (slabs and walls Width): B#18 = 6.50 m

Equal Spacing Hinges configuration (width approximately equals beam height)

Figure 3. Frame FEM model for Buildings #18. Frame sections (left), Hinges Configuration (right)

Plastic Hinges Variants

As commented previously, the hinges adopted for pushover were defined according to ASCE 41-17, and works well for pseudo-static analysis, however for time-history analysis this option cannot be the best choice. Nonlinear analysis of reinforced concrete structures subjected to seismic loads requires an accurate representation of stiffness degradation. In SAP2000, the Fiber P-M2-M3 model enables a detailed response of materials by defining nonlinear stress-strain relationships for both concrete and steel. To assess the sensitivity of stiffness degradation, different parameter variants were analyzed, as presented in Table 1.

Table 1: Fiber hinges stiffness-degradation parameters and variants.

Parameter	Baseline	Variant 1	Variant 2	Variant 3
Final Compression Slope (Concrete)	-0.1·E	-0.2·E	-0.3·E	-0.25·E
Hysteresis Model (Concrete)	Takeda	Takeda	Degrading	Takeda
Ultimate Strain Capacity (Concrete)	0.005	0.004	0.0035	0.0045
Strain at Peak Strength (Concrete)	0.002286	0.0020	0.0018	0.0021
Hysteresis Model (Steel)	Kinematic	Isotropic	Isotropic	Kinematic
Strain at Onset of Strain Hardening (Steel)	0.01	0.008	0.007	0.009
Ultimate Strain Capacity (Steel)	0.09	0.08	0.07	0.085
Final Slope Multiplier (Steel)	-0.1·E	-0.2·E	-0.25·E	-0.15·E
Name	NL_Fiber	NL_Fiber2	NL_Fiber3	NL_Fiber4

To complement the Baseline fiber model (NL_Fiber), we introduced three additional variants (NL_Fiber2, NL_Fiber3, and NL_Fiber4), each adjusting the hysteresis and strain capacity for concrete and steel:

- **Baseline** (NL_Fiber): Uses a Takeda model [Takeda et al] for concrete and kinematic hardening in steel. Although suitable for moderate ductility scenarios, it may underestimate stiffness loss under high-cyclic demands.
- **Variation 1** (NL_Fiber2): Retains the Takeda concrete model but switches steel to isotropic hardening and reduces concrete ductility. This increases cyclic stiffness degradation and promotes earlier steel yielding, improving energy dissipation.
- **Variation 2** (NL_Fiber3): Adopts a more aggressive Degrading model for concrete, along with isotropic steel. This simulates worst-case stiffness reduction suitable for high-seismic-demand regions, albeit with more brittle concrete behaviour.
- **Variation 3** (NL_Fiber4): A balanced approach that maintains Takeda for concrete and kinematic steel, but slightly elevates the softening rate. It preserves enough ductility while introducing additional post-peak degradation.

By comparing the baseline to these three variants, we aim to gauge how progressive adjustments in softening slopes, hysteresis models, and strain capacities affect the local and global seismic response.

Time-History Setup

A modal-based approach was adopted for the time-history analyses, extracting up to 200 eigenmodes with a frequency cutoff of 50 Hz. The resulting mode shapes were used to capture the structure's principal dynamic characteristics. A small convergence tolerance ($1e-9$) was enforced in the modal solution to ensure numerical stability.

For the linear transient analysis, we ran 2,448 output steps at a time step size of 0.01 s. During the first 4 seconds, a ramp function gradually applied dead loads to minimize initial oscillations. Rayleigh damping was defined to achieve 7% damping at two reference frequencies (0.769 Hz and 13 Hz), yielding proportional mass and stiffness coefficients ($\alpha \approx 0.637$, $\beta \approx 1.618e-3$).

Subsequently, in the nonlinear regime, we introduced a separate load case (Dead_NL) with geometric nonlinearity (P-Delta). This state served as the starting point for the direct-integration time-history solution, which included large-displacement effects. A total of 2,048 output steps were computed at $\Delta t = 0.01$ s, maintaining the same Rayleigh damping scheme. To handle nonlinearities in each step, SAP2000's Hilber-Hughes-Taylor integration ($\alpha = -0.1$, $\gamma = 0.6$, $\beta = 0.3025$) was used in conjunction with an iterative-only solver. Up to 200 Newton-Raphson iterations were allowed per step, enhanced by line-search techniques (maximum 20 tries, acceptance tolerance 0.1, step factor ~ 1.2) to improve convergence. A minimum substep size of $1e-6$ was set to guard against abrupt stiffness changes, while the maximum substep was capped at 0.01 s. Convergence tolerances of $1e-3$ to $1e-4$ (relative) ensured the solution closely followed the prescribed force-deformation path at each stage of loading.

RESULTS

Global Response

Figure 4 (left) compares the base shear time histories for the linear elastic solution and the various nonlinear models at $\xi=7\%$. As expected, the Fiber-based hinges exhibit greater energy dissipation, lowering peak base shear relative to the baseline NL model. This effect is most pronounced after about 12 seconds, where higher stiffness degradation in the Fiber variants diminishes residual oscillations. By contrast, the difference among the Fiber variants themselves remains modest.

Figure 4 (right) shows the damping sensitivity in the baseline model ($\xi=4\%-7\%$). Little variation is seen across these damping values, implying that plasticity dominates the system's energy dissipation. A similar trend emerges in Figure 5 (left and right), where the top displacement time histories are only slightly affected by changes in damping, further reinforcing that inelastic hinge action drives the overall response.

From these results, an approximate behavior factor (q) can be derived by comparing elastic and non-linear base shear. Table 2 lists q -factors for each non-linear model at $\xi=7\%$. Despite some variance in stiffness degradation among the Fiber hinges, the range of q stays in the 1.69–1.75 corridor, with the baseline NL case at 1.43. Table 3 summarizes how damping adjustments (3%-7%) affect q in the baseline non-linear model. Again, minimal sensitivity is observed, indicating that double counting of damping is not a major concern in this conceptual study. Overall, the NL Fiber variants average $q = 1.71 (\pm 0.07)$, slightly higher than the baseline’s 1.43, underlining the role of distributed plasticity and enhanced energy dissipation in the Fiber approach.

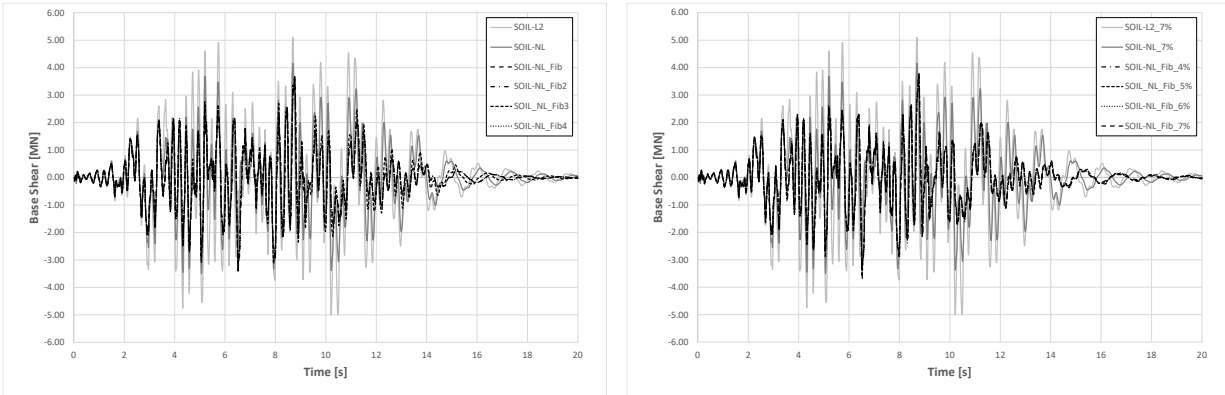


Figure 4. Base shear vs. time for linear elastic and non-linear models. Left: Results for different models ($\xi = 7\%$). Right: Effect of damping ratio in the baseline model ($\xi = 4-7\%$).

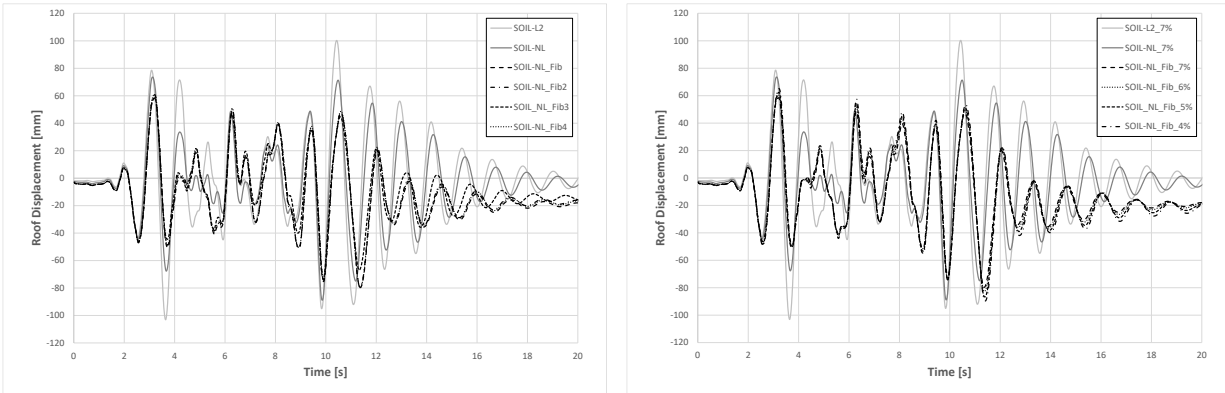


Figure 5. Top displacement vs. time for linear elastic and non-linear models. Left: Results for different models ($\xi = 7\%$). Right: Effect of damping ratio in the baseline model ($\xi = 4-7\%$).

Table 2: Behavior Factor obtained from Base shear forces for different non-linear models ($\xi = 7\%$).

Model	NL	NL_Fib	NL_Fib2	NL_Fib3	NL_Fib4
q	1.43	1.69	1.69	1.75	1.69

Table 3: Behavior Factor obtained from Base shear forces for the baseline non-linear model ($\xi = 4-7\%$).

Damping	3%	4%	5%	6%	7%
q	1.60	1.69	1.63	1.78	1.68

Local Demand Ratios

Figure 6 presents the elements where the local behavior was analyzed, for beams negative and positive bending moments, together with shear forces at the ends, whereas for columns the bending moments and shear forces at the bottom and the top. Tables 4 to 8 summarizes the behavior factor obtained for each non-linear model, presenting the mean, maximum and minimum value of q . It is important to note that those cases in which $q < 1$ implies that non-linear analysis produces greater internal forces than the elastic analysis. Although the design based in elastic internal forces implies different safety factors, it is evident that the zones in which bending moments increase is possible, due the non-linear analysis respect this capacity, however for shear forces that exceed the elastic ones, it can be a problem, that require redesign this element. As expected, important redistribution of bending moments occurs in the horizontal elements, where the increase of negative moments is accompanied of a reduction of the positive moments, that it is clearly reflected in the behavior factors obtained. As indicated in the global analysis, the baseline and the variants do not reflect significant differences, producing the variant 3 the greater values of q . On the other hand, in the columns located on the left in Figure 6, the values of q , are lower than 1 for bending and shear forces, it must be clarified that these occurs only for NL case, as can be seen in Tables 7 and 8.

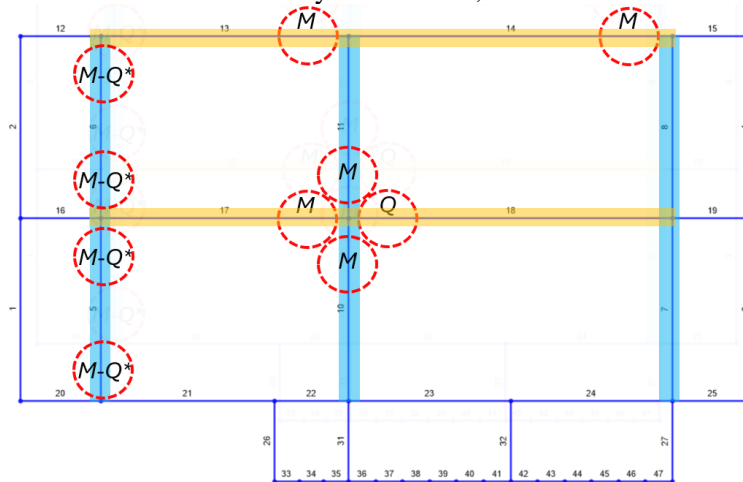


Figure 6. Local Demand Analysis: Elements studied and critical zones where $q < 1$.

Table 4: Behavior Factor obtained from Negative Bending moments in beams ($\xi = 7\%$).

Model	NL	NL_Fib	NL_Fib2	NL_Fib3	NL_Fib4
Max q	1.54	2.21	2.17	2.57	2.17
Min q	0.62	0.67	0.67	0.64	0.67
Avg q	1.00	1.12	1.11	1.15	1.12

Table 5: Behavior Factor obtained from Positive Bending moments in beams ($\xi = 7\%$).

Model	NL	NL_Fib	NL_Fib2	NL_Fib3	NL_Fib4
Max q	1.63	2.05	2.01	2.03	2.04
Min q	1.04	1.10	1.09	1.10	1.09
Avg q	1.26	1.47	1.46	1.47	1.47

Table 6: Behavior Factor obtained from Shear forces in beams ($\xi = 7\%$).

Model	NL	NL_Fib	NL_Fib2	NL_Fib3	NL_Fib4
Max q	1.78	2.51	2.57	2.62	2.58
Min q	0.64	0.70	0.70	0.69	0.70
Avg q	1.46	1.89	1.87	1.87	1.88

Table 7: Behavior Factor obtained from Bending moments in columns ($\xi = 7\%$).

Model	NL	NL_Fib	NL_Fib2	NL_Fib3	NL_Fib4
Max q	1.54	2.25	2.23	2.57	2.25
Min q	0.92	1.25	1.22	1.25	1.24
Avg q	1.15	1.62	1.60	1.64	1.61

Table 8: Behavior Factor obtained from Shear forces in columns ($\xi = 7\%$).

Model	NL	NL_Fib	NL_Fib2	NL_Fib3	NL_Fib4
Max q	1.55	2.45	2.43	2.53	2.46
Min q	0.89	1.11	1.10	1.15	1.10
Avg q	1.16	1.62	1.61	1.64	1.61

Hinge Formation and Ductility

Figure 7 shows the final hinge states for both the baseline NL model and the Fiber variants, while Figure 8 illustrates reinforcement strain profiles in critical sections (here depicted for the NL_Fiber4 case). In the baseline model, hinges generally remain within an Immediate Occupancy (IO) range, whereas the Fiber hinges shift toward a state beyond the Collapse Prevention (CP) limit. In SAP2000 when a hinge is reported to be in the “E” state, it means the deformation demand has surpassed the code’s threshold for collapse prevention, indicating severe damage and potentially near-failure behavior. Nevertheless, Figure 8 confirms that the reinforcing steel provides enough residual capacity to avert collapse, even under those more advanced damage states.

Earlier parametric expectations suggested distinct divergence among the Fiber variants. However, the actual computations reveal relatively similar overall responses—though each variant does reflect its respective degree of stiffness degradation. In line with prior reasoning, more aggressive degradation (Variant 2) leads to faster stiffness loss but preserves global stability, isotropic hardening in steel (Variants 1 and 2) yields enhanced cyclic behavior, and adjusting concrete strain limits affects local demand distributions. Despite these nuances, the overall variation in results remains modest.

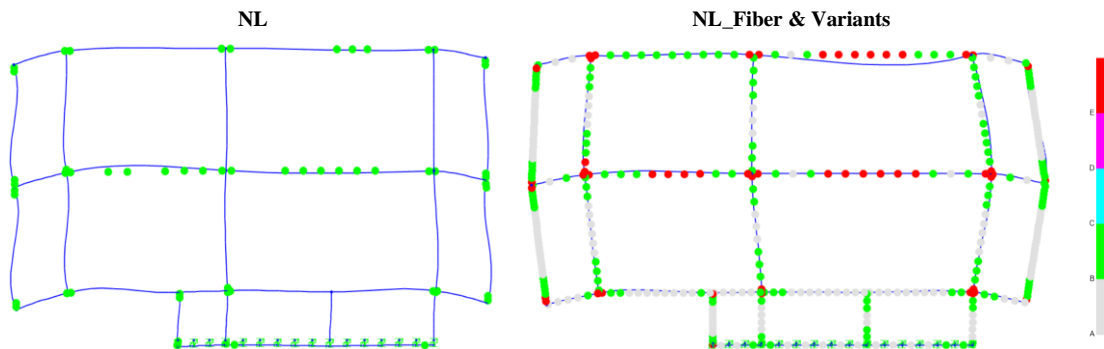


Figure 7. Final hinge configuration

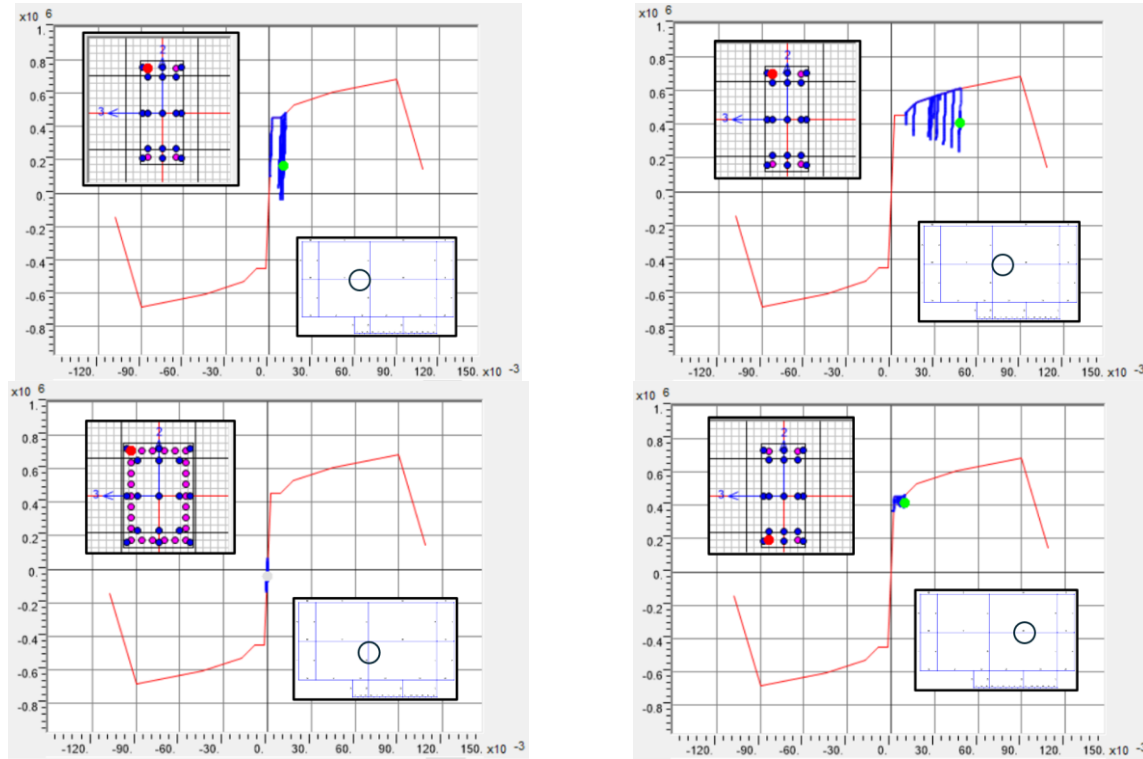


Figure 8. Stress (kN/m^2) vs Reinforcement steel strains in critical sections (NL_Fiber4 load case)

CONCLUSIONS

The primary objective of this study was to validate the behavior factor (q) used in the conceptual seismic design of RC buildings for the ITER project, extending the prior pushover-based approach with detailed time-history analyses.

Comparison to Pushover Analysis

- When the same hinge definitions employed in static (pushover) analyses are applied to dynamic time-histories, the average q -factors are broadly consistent.
- However, certain members exhibit $q < 1$ in localized bending or shear demands, emphasizing the need for special design checks in specific zones.

Role of Fiber Models

- Fiber-based hinges with varying degradation offer a robust mechanism to simulate cyclic loading and progressive stiffness loss.
- Despite testing multiple parameter variants (baseline, plus three modifications), global behavior factors vary only modestly.
- Nonetheless, fiber models systematically yield higher q -values than the baseline NL hinges, reflecting enhanced energy dissipation due to distributed plasticity.

Double Counting of Damping

- A parametric study altering Rayleigh damping from 3% to 7% reveals limited sensitivity in the non-linear results.
- This finding suggests plastic deformation dominates total energy dissipation, reducing concerns about overestimating damping at the conceptual design stage.

Implications for Seismic Design

- For conceptual-level RC building design, non-linear time-history validations—like those presented here—help confirm whether a chosen q -factor is safe.

- In advanced design phases, regions where $q < 1$ highlights local inelastic force redistributions that may demand refined detailing or alternative design solutions.
- Future work may refine material hysteresis and fiber modeling or compare with experimental data to solidify these findings.

In conclusion, time-history analyses largely corroborate the pushover-based q but expose local ductility demands that linear approaches may overlook. The proposed fiber models enhance realism by accounting for degradation and cyclic effects, yet the global q -factor remains relatively insensitive to the specific variants tested—allowing confidence that a $q \leq 2$ is appropriate at this conceptual design stage.

REFERENCES

- Ezeberry Parrotta, J. I., G. Hanna, D. Combescure. “*Pushover Analysis and Conceptual Design of RC Frames – Challenges in Seismic Design for Nuclear Facilities.*” SMiRT-28, Toronto, Canada a0-15, 2025.
- P-CARES: “*Probabilistic Computer Analysis for Rapid Evaluation of Structures (NUREG/CR-6922).*” Brookhaven National Laboratory, U.S.NRC, 2007.
- Idriss, I. M., J. I. Sun: “*User’s Manual for Shake-91: A Computer Program for Conduction Equivalent Linear Seismic Response Analyses of Horizontally Layered Soil Deposits.*” Center for Geotechnical Modeling, Department of Civil & Environmental Engineering, University of California, 1992.
- I-LSSR. “*Load Specifications for Buildings with Safety Requirements,*” (IDM: 2ERTXQ v3.3). ITER.
- NUREG 0800: Section 3.7.1. “*Seismic Design Parameters.*” U.S.NRC, 2007.
- RG 1-208: “*A Performance-Based Approach to Define the Site-Specific Earthquake Ground Motion.*” U.S.NRC, 2007.
- I-SDCB. “*ITER Structural Design Code for Buildings (I-SDCB) - Part1: Design Criteria,*” IDM: 283B24 v3.0
- I-SIR. “*ITER Project - Site Investigation Interpretative Report - Phase 1 and 2,*” IDM: 2M3XEC v1.3
- RG 1.61: NRC Regulatory Guide on Damping Values for Seismic Design of Nuclear Power Plants, U.S. Nuclear Regulatory Commission.
- SAP2000 Structural Analysis Software, Version 25.1, Computers and Structures, Inc.
- ASCE 41-17: “*Seismic Evaluation and Retrofit of Existing Buildings,*” American Society of Civil Engineers (ASCE), Reston, VA.
- Takeda, T.; M. A. Sozen, and N. N. Nielsen, “*Reinforced Concrete Response to Simulated Earthquakes,*” J. Struct. Engrg. Div., ASCE, Vol. 96, No. 12, pp. 2257–2273. 1970.
- ATC-40: “*Seismic Evaluation and Retrofit of Concrete Buildings,*” Applied Technology Council (ATC). 1996.
- Eurocode 2: “*Design of Concrete Structures – Part 1: General Rules and Rules for Buildings (EN 1992-1-1),*” European Committee for Standardization (CEN), Brussels.
- Eurocode 8: “*Design of Structures for Earthquake Resistance – Part 1: General Rules, Seismic Actions and Rules for Buildings (EN 1998-1).*” European Committee for Standardization (CEN), Brussels.